

Introduction, revelation, and evolution of complementary gratings in photorefractive bismuth silicon oxide

M. C. Bashaw, T.-P. Ma, R. C. Barker, and S. Mroczkowski
*Department of Applied Physics, Department of Electrical Engineering,
 and Center for Microelectronic Materials and Structures, Yale University,
 New Haven, Connecticut 06520-2157*

R. R. Dube

*IBM Research Division, Thomas J. Watson Research Center,
 P.O. Box 704, Yorktown Heights, New York 10598*

(Received 2 March 1990)

Principal and complementary space-charge gratings are formed in photorefractive bismuth silicon oxide with use of 785-nm light. An electric field is optionally applied in the direction of the grating for hologram evolution by either drift or diffusion of charge carriers. For write times on the order of the decay time of the principal grating, no complementary behavior is observed. For much longer write times, a complementary space-charge grating is introduced both in the presence and in the absence of the applied field, and is initially hidden due to screening by the principal grating. Uniform illumination in the presence of the field reveals the complementary grating. Time-resolved data show its growth and decay, with a response rate much lower than that of the principal grating. A two-level electron-hole transport model explains the observations; one level participates in the establishment of the principal grating by majority carriers, and the other in the establishment of the extended-lifetime complementary grating by minority carriers. A scheme for multiplexing normal and extended-lifetime complementary gratings is presented.

I. INTRODUCTION

The photorefractive effect generates holographic gratings in bismuth silicon oxide ($\text{Bi}_{12}\text{SiO}_{20}$), known also as BSO, by redistribution of charge between states within the energy band gap. Several studies have revealed the energy levels of some of these states.¹⁻⁶ BSO has been shown to have a direct band gap of 3.25 eV, with electron-filled electrically neutral states situated at about 0.65 eV above the valence band; these states participate in the photoexcitation required for the photorefractive process. A photoluminescence center has been identified at 1.95 eV above the valence band.¹ As many as eight electron-trap states of depths up to 1.4 eV (from the conduction band) have been identified in BSO by thermally-stimulated-current analysis.² Wavelengths near 500 nm (blue-green light) are best suited and most commonly used for writing holographic gratings in BSO.

Detailed accounts of the photorefractive process may be found elsewhere.⁷⁻¹¹ Briefly, two plane waves of wavelength λ intersecting at an angle 2θ generate a periodic interference pattern,

$$I = I_0 [1 + m \operatorname{Re}(e^{ikx})], \quad (1)$$

where I_0 is the total intensity, \hat{x} is the direction of the grating, m is the interference modulation factor, $\mathbf{k} = (2\pi/\Lambda)\hat{x}$, and $\lambda = 2\Lambda \sin\theta$, where Λ is the grating period. Figure 1 shows \hat{x} , \mathbf{k} , and 2θ . Electrons are photoexcited into the conduction band in higher concentrations within the regions of constructive interference, and

diffuse into the regions of destructive interference, where they relax to empty states in the energy band gap. The resultant periodic space-charge pattern may be described approximately by its lowest-order Fourier harmonic as

$$E = E_0 + \operatorname{Re}(E_{\text{SC}} e^{ikx}), \quad (2)$$

where E_0 is the applied field and E_{SC} is the space-charge field. This field modulates the index of refraction

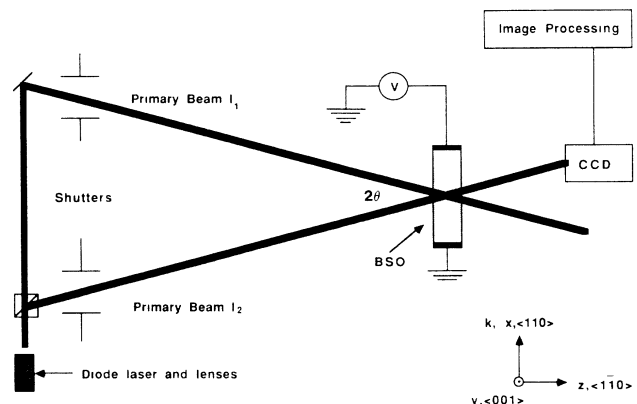


FIG. 1. Experimental arrangement for holographic recording in BSO at 785 nm. $I_1 = 665 \mu\text{W}/\text{cm}^2$ and $I_2 = 490 \mu\text{W}/\text{cm}^2$. Grating period $\Lambda = 10 \mu\text{m}$. $E_0 = 0$ or 5 kV/cm. Note shown is a shutter-controlled 514.5-nm beam of an argon laser, incident on the surface of the crystal.

through the electron-optic effect, creating a diffraction grating. The space-charge accumulation limits the diffusion process, much like the charge-depletion region in a p - n junction in semiconductors. Application of a high electric field in the direction of the grating introduces drift and competes with the space-charge accumulation, enhancing the effect.

The diffraction grating is a simple hologram and may be read by a probe beam of any wavelength which is Bragg-matched to the grating, including either write beam; the scattered beam has a diffraction efficiency

$$\eta \propto |E_{SC}|^2. \quad (3)$$

The gratings are erased by uniform illumination of the crystal. Write-and-erase sequences are typically characterized by simple-exponential behavior. For the case of diffusion only (no electric field) and a large grating period (at least 10 μm in BSO) the space-charge-grating decay time is simply the dielectric relaxation time of the crystal,

$$\tau = \epsilon\epsilon_0/\sigma, \quad (4)$$

where ϵ_0 is the permittivity of free space, ϵ is the relative permittivity, and σ is the conductivity. In BSO, τ increases with decreasing grating period and increasing electric field, to saturation in both cases.

This paper presents data which demonstrate the generation of photorefractive gratings and a sequence for extending grating lifetimes with 785-nm light in nominally undoped BSO. Outside of the blue-green range, photorefractive-grating enhancement has been observed by preillumination with infrared light,¹² gratings have been written in undoped BSO with 632.8-nm light,^{13,14} and grating decays have been observed with 820-nm light for gratings written with 514.5-nm light,¹⁵ but this is believed to be the first study of grating generation by infrared light in BSO.

Recently, the formation of extended-lifetime holograms, known also as read-only, fixed,¹⁶ semipermanent,¹⁷ and quasinondestructive⁴ holograms, has received much attention. Herriau and Huignard demonstrate a multiple-step sequence for generating extended-lifetime complementary gratings using both 514.5-nm primary and 632.8-nm probe beams.^{4,16} Attard uses a similar process for grating restoration.¹⁸ Arizmendi reports a thermal fixing process for gratings generated with 632.8-nm primary beams, apparently involving grating compensation by mobile ions.¹³ Vainos *et al.* describe semipermanent holograms resulting from the photochromic effect.¹⁹ Additional methods for extending the lifetime of holograms have been identified in other photorefractive crystals.^{20–24}

The sequence described in this paper is a two-step process for introducing and then revealing extended-lifetime complementary gratings in BSO using 785-nm illumination. A two-level electron-hole-transport model accounts for the observations.

II. EXPERIMENTAL DETAILS

Single-crystal boules are grown by Czochralski pulling from a stoichiometric melt.^{25,26} The dimensions of

the cut crystal are $10 \times 7 \times 2 \text{ mm}^3$ for the $[001] \times [110] \times [1\bar{1}0]$ lattice directions, respectively, as shown in Fig. 1. Silver-paint electrodes are used to make electrical contact with the crystal.

The experimental setup is shown in Fig. 1. Light from a Sharp diode laser (model LT021MF0) operating at 10 mW with a wavelength of 785 nm is collimated and directed through a beam splitter. The two primary beams pass through computer-controlled electromechanical shutters. Both beams are directed to the $[110]$ face of the BSO crystal, where they create an interference pattern within the volume of the crystal. The grating vector points along the $[110]$ direction, and an electric potential of up to 3.5 kV may be applied between opposite (110) planes. The gratings are written with both shutters open, 665 and 490 $\mu\text{W}/\text{cm}^2$ illumination,²⁷ and erased with only one shutter open, 665 $\mu\text{W}/\text{cm}^2$ illumination. The image beam is detected by a 512×512 picture-element (pixel) array, computer-controlled CCD camera (CCD denotes charge-coupled device); each pixel has a digital gray scale from 0 to 255. When the image beam is blocked, the grating can be detected with the reference beam, now serving as a probe beam. This arrangement does not permit continuous monitoring of grating formation, but does allow such monitoring of grating decay.²⁸ Because of signal-to-noise considerations, no two-beam coupling is observed with the current arrangement. Not shown in the figure is a 514.5-nm beam used to erase any residual grating between events.

For electric potential V and distance d the applied electric field is represented by $E_V = cE'_0$, where $E'_0 = V/d$ and c ranges from $\frac{1}{3}$ to 1, as shown in the literature.^{29,30} Here, $d = 7 \text{ mm}$. The value of c for $V = 3.5 \text{ kV}$ is estimated by examining the relative diffraction efficiency as a function of electric field for photorefractivity at 514.5 nm and a grating spacing of 1 μm , as follows.³¹ For little trap filling, the space-charge field is

$$E_{SC} = -m(E_0 + iE_D), \quad (5)$$

where $E_D = kk_B T/e$, and E_0 is the electric field applied in the grating direction. Thus,

$$\eta(E_0 = E_V)/\eta(E_0 = 0) = (E_V^2 + E_D^2)/E_D^2. \quad (6)$$

For a 1- μm grating, $E_D \approx 1.5 \text{ kV}/\text{cm}$, $\eta(E_0 = E_V)/\eta(E_0 = 0) \approx 2$, and, therefore, $c \approx \frac{1}{3}$.

III. RESULTS

A write-erase curve is generated in the following manner. Any existing grating is completely erased with 514.5-nm illumination between events. This erasure wavelength has been chosen for convenience only; any broadband source with significant illumination near or below 514.5 nm would be adequate. Gratings are written for successively longer time periods, measured, and then erased until saturation diffraction efficiency is achieved. The measured diffraction efficiencies are then assembled into one write curve. The erase portion is generated more routinely as a grating is read by a uniformly illuminating the reference beam and, thus, the decays. A

typical write-erase curve is shown for $E'_0 = 5$ kV/cm in Fig. 2. Although the decay slightly deviates from a simple exponential, the decay time of the diffraction efficiency, $\tau/2$, is estimated to be 15 sec, and the decay-energy density, $S_d = \tau I$, is estimated to be 20 mJ/cm², where I is the erase-beam intensity.

According to photorefractive theory, $\eta \propto 1/\Lambda^2$ for the case of diffusion only.⁷⁻¹¹ Consequently, the diffracted image at 10 μm is 100 times weaker than at $\Lambda = 1$ μm and, for this case, could be detected only by visual inspection of the CCD camera display, thereby precluding quantitative analysis. Nevertheless, the dielectric relaxation rate, $\Gamma = \tau^{-1}$, is estimated by writing a grating with the applied potential and then erasing it with no applied potential. In this case, $\tau/2 \approx 1$ sec and $S_d \approx 1.4$ mJ/cm². The relaxation rate and, therefore, the photoconductivity at 785 nm are approximately 25 times lower than those at 514.5 nm for equal light intensities, or approximately 40 times lower for an equal rate of photon incidences.

For exposures well beyond the minimum time needed to saturate the diffraction efficiency, the field-enhanced decay of the diffraction efficiency exhibits some peculiar effects. Again, the grating period is 10 μm . Throughout the decay process, the reference probe beam and applied electric potential are maintained at constant levels. For this situation the grating-decay process consists of three regimes, as shown in Fig. 3. First, the grating decays at approximately the same rate as for the case of minimum saturation exposure time. Next, the grating partially recovers. Finally, it decays at a rate approximately 150 times slower than the initial decay rate. The grating initially observed is the principal grating, and the grating subsequently revealed is the complementary grating patterned after the first. At any time during the process the grating can be completely erased by uniform illumination at 514.5 nm with no possibility for recovery. The

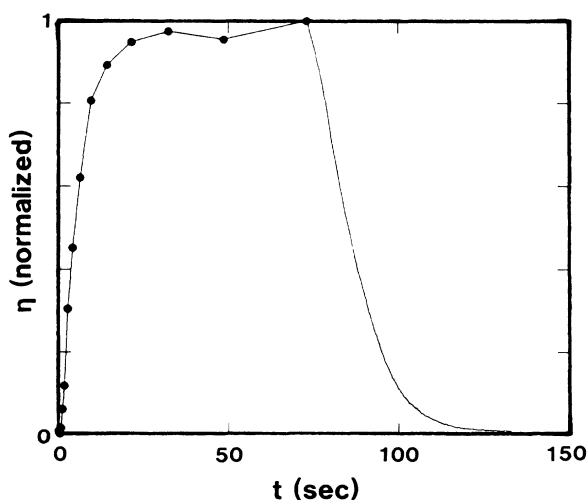


FIG. 2. Write-and-erase evolution of diffraction efficiency, η . $E'_0 = 5$ kV/cm, $\lambda = 785$ nm, and $\Lambda = 10$ μm . For the write portion of the curve, up to 75 sec, the points are assembled from different write events. The erase portion, after 75 sec, is taken from one erasure.

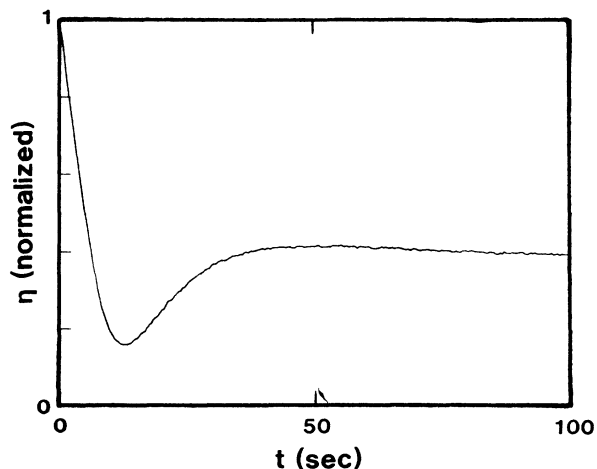


FIG. 3. Typical decay of the diffraction efficiency for write periods several times longer than the grating time constant. Here the write time is 900 sec. The grating initially decays with approximately the same time constant as that in Fig. 2, then experiences partial recovery. The residual grating decays at about 150 times the grating time constant. $E'_0 = 5$ kV/cm, $\lambda = 785$ nm, $\Lambda = 10$ μm , $I_1 = 665$ $\mu\text{W}/\text{cm}^2$, and $I_2 = 0$.

recovery strength of the grating varies from decay to decay; this may be related to fluctuations in grating strengths for high applied electric fields, apparently due to a random running grating effect.^{32,33}

For the case of writing with no field, a similar recovery effect occurs leading to a reproducible process for extending the lifetime of a hologram. The same crystal geometry is used, and the grating period remains at 10 μm . For exposures well beyond the minimum exposure time needed to achieve the diffusion field, the following sequence produces the extended-lifetime hologram. With no applied electric potential, a space-charge grating is written into the BSO crystal (by exposure to both primary beams). As mentioned above, the resultant diffusion grating is too weak to be monitored quantitatively. Application of an electric potential of 3.5 kV during erasure (by exposure to only one primary beam) results in the decay of the principal grating, revealing a very strong complementary grating, orders of magnitude stronger than the initial net diffusion grating. For longer exposure times, the revealed grating is stronger, and eventually reaches saturation. The gratings saturate at a strength within 90% of a corresponding grating which can be written with 3.5 kV. The revelation time evolution is shown in Fig. 4. The revealed complementary grating decays at a rate approximately 150 times slower than the revelation rate and at approximately the same rate as the residual grating discussed in the preceding paragraph; this decay rate is also 150 times slower than the decay rate for a grating written at the revelation potential in the ordinary manner. Figure 5 shows a series of such curves for different write times. The grating is completely erased with uniform illumination at 514.5 nm between each hologram sequence. Figure 6 is a summary of Fig. 5, showing the write time needed to achieve a partic-

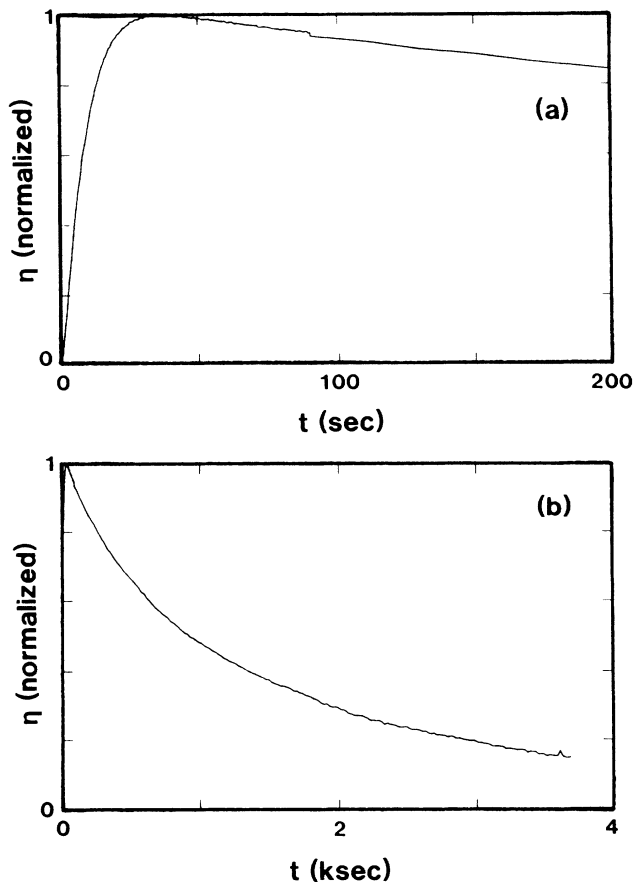


FIG. 4. (a) Revelation sequence for hologram fixing. The zero-potential write time is 640 sec. $E'_0 = 5$ kV/cm, $\lambda = 785$ nm, $\Lambda = 10$ μ m, $I_1 = 665$ μ W/cm², and $I_2 = 0$ for the revelation sequence. The revelation rate is approximately the same as the grating write-erase rate. (b) Decay of residual grating. This decay rate is approximately 150 times slower than the revelation rate.

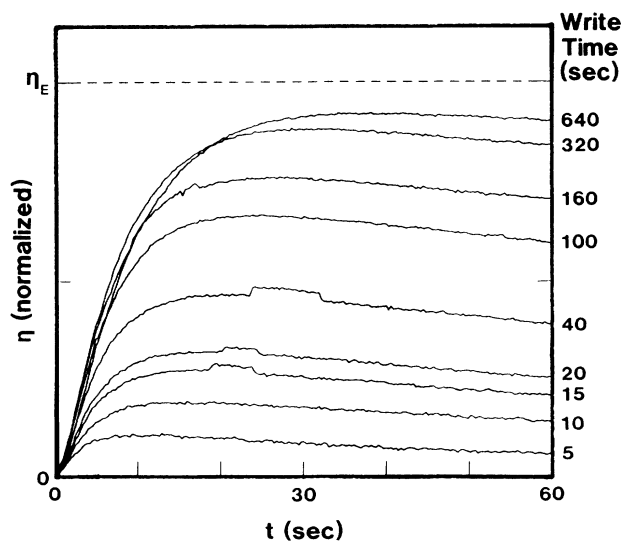


FIG. 5. Revelation sequences for different write times. Complementary gratings are written without applied potential for different time periods, as indicated. The peak diffraction efficiency obtained in Fig. 2 is indicated as η_E . $E'_0 = 5$ kV/cm, $\lambda = 785$ nm, $\Lambda = 10$ μ m, $I_1 = 665$ μ W/cm², and $I_2 = 0$ for the revelation sequence.

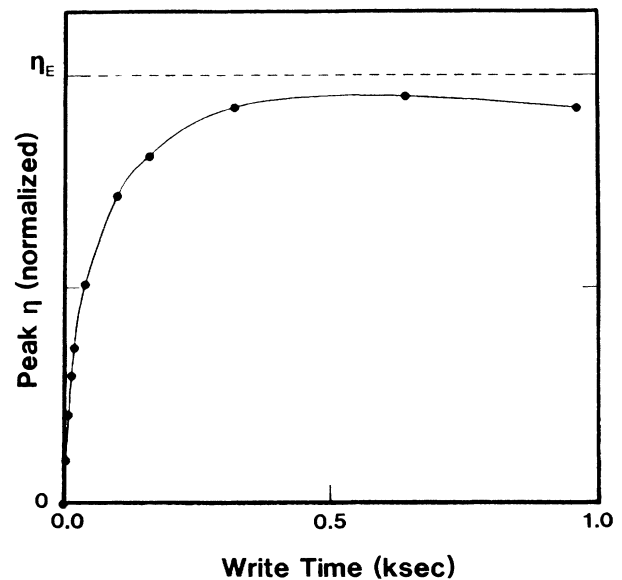


FIG. 6. Write time needed to achieve a particular diffraction efficiency in the revelation sequences shown in Fig. 5. The points are determined by linearly extrapolating the decay of the complementary grating to $t = 0$.

ular diffraction efficiency of a revealed grating.

If at anytime during this process the applied potential is turned off, the net grating decays to zero, but may be restored by reapplication of the potential. No net grating is detected, but principal and complementary gratings, now hidden, still exist. Continuous illumination with no applied potential and occasional revelation in the manner described in the preceding paragraph show that the complementary gratings are eventually erased, with a decay rate 1000 times slower than the estimated dielectric relaxation rate.

IV. DISCUSSION

The observations may be explained by an electron-hole-transport process, involving two different sets of levels in the energy-band gap as described by Kukhtarev *et al.*³⁴ and Valley.³⁵ Figure 7 shows the model. The set used for electron transport consists of N total states composed of filled states of density N^- and empty traps of density N^+ ; space-charge accumulation occurs by the transfer of electrons from filled to empty states. The set used for hole transport consists of P total states composed of electron-filled states, P^- , and empty (or hole-filled) states, P^+ ; space-charge accumulation here occurs by the transfer of holes from empty to filled states.³⁶ Compensating ions are present to ensure that the system is overall charge neutral; thus, the superscripts do not necessarily represent the charge state of a particular level.³⁷

Photoconductivity of undoped BSO has been shown generally to be of n type (see Ref. 1 and 43), and thus $\sigma_e \gg \sigma_h$, where σ_e and σ_h are the electron and hole photoconductivities. Although the relevant quantities have yet to be measured, the photoconductivity at 785 nm in

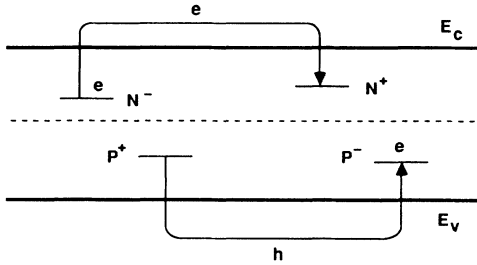


FIG. 7. Electron-hole-transport model utilizing two sets of levels in the energy-band gap.

BSO is taken as n type and the dielectric limit is assumed for the discussion that follows. Two-beam-coupling studies are best suited for determining the relevant quantities, but are not possible here because of signal-to-noise constraints. For the case of p -type photoconductivity, the roles of electrons and holes must be interchanged, but the underlying physics remains the same.

Using the model, the charge redistribution for the diffusion case may be described by three phases. First, for minimal charge transfer within both levels, N and P , the coefficient of the space-charge field in Eq. (2), E_{SC} , is diffusion-limited and is, in general, dependent on σ_e , σ_h , and k . For small k and minimal state filling, E_{SC} becomes the diffusion-limited field and may be taken as

$$E_{DL} = -imE_D(\sigma_e - \sigma_h)/(\sigma_e + \sigma_h). \quad (7)$$

This is the dielectric limit of the system and is equivalent to the similar limit for single-level electron-hole transport.³⁵

Using one set of partially filled energy levels in the band gap, the majority carrier establishes a diffusion-limited grating relatively quickly, and saturates when the space-charge field prohibits further charge accumulation. For n -type BSO, electron transport dominates, and the resultant expression for the diffusion-limited field becomes

$$E_{DL} = -imE_D, \quad (8)$$

and the space-charge field is $E_{SC} = E_{DL}$. This is the principal, electron-formed grating.

The next phase involves minority-carrier transport using a second set of levels. After the electron transport establishes the principal grating, regions of accumulated negative charge repel electrons and thus prevent further accumulation of net charge. Holes, however, are *attracted* by the regions of accumulated negative charge. Therefore, both photoexcited and possibly thermally excited holes diffuse and drift under the influence of the diffusion field into the regions of highest electron concentration, where they relax to states in the band gap. Because electrons have higher photoconductivity, they will continue to migrate to these regions to compensate for hole screening, but at a slower rate to preserve the amplitude of the space-charge field.

The resultant electron-hole transport is a field-assisted ambipolar diffusion process. In the limiting case that $\sigma_e = \sigma_h$, no space-charge field will be established, as indi-

cated by Eq. (7), and normal ambipolar diffusion will occur. In this manner, large numbers of charge carriers migrate, creating large, complementary space-charge gratings of nearly equal amplitude but opposite sign, whose net field is the diffusion-limited space-charge field. In semi-insulating InP, a screening effect of similar physical origin has been observed by Nolte *et al.*: At low temperatures, the formation of complementary gratings results in the weakening of the photorefractive effect.³⁸ The net space-charge field is described as a superposition of two fields,

$$E_{SC} = -iE_e + iE_h, \quad (9)$$

where $E_h \geq 0$ is the amplitude of the π -shifted hole-created field resulting from second-phase hole transport and $E_e = |E_{DL}| + E_h \geq 0$ is the amplitude of the electron-created field resulting from first- and second-phase transport, and, as before, $E_{SC} = E_{DL}$.

In the final phase, trap filling becomes substantial, and the process reaches steady state. Here,

$$E_{SC} = -imE_D(E_{qe} - E_{qh})/(E_{qe} + E_{qh} + E_D), \quad (10)$$

where $E_{qe} = eN^-N^+/\epsilon\epsilon_0kN$ and $E_{qh} = eP^-P^+/\epsilon\epsilon_0kP$ are the limiting space-charge fields for the electron- and hole-transport systems, respectively.³⁵ For $E_{qe} \gg E_{qh}$, which may be the case in BSO, again $E_{SC} = E_{DL}$, and the expressions for the complementary space-charge fields are identical to those in phase two. For the revelation sequences in Fig. 5, which do not reach the maximum attainable value, the charge-transfer process has not reached steady state and, therefore, has stopped during the second phase.

The revelation process occurs as follows. When the grating is illuminated uniformly under the application of a high electric field, the effects of diffusion may be neglected. Electrons and holes are photoexcited, drift in opposite directions, and become evenly redistributed, thus erasing each grating. The electron-formed grating is erased first due to the higher photoconductivity of electrons, revealing the hole-formed grating, which decays more slowly, by a factor of 150. The expression for the net space-charge grating decay is

$$E_{SC}(t) = -iE_e \exp(-\Gamma_e t) + iE_h \exp(-\Gamma_h t), \quad (11)$$

where Γ_e and Γ_h are the high-field grating-decay rates for the electron- and hole-transport systems, respectively. For $\Gamma_e \gg \Gamma_h$, E_{SC} is initially E_{DL} , vanishes a short time later at time $t_1 \ll \Gamma_e^{-1}$, reaches a maximum at E_h after a few time constants Γ_e^{-1} , and then decays to zero at the slower rate Γ_h^{-1} . In the data presented here, the initial decay would not be detected because of unsuitable signal-to-noise ratio.

Unlike the decay of the grating field, the decay of the diffraction efficiency is expected to deviate from a simple difference of exponentials as

$$\eta \propto |E_e \exp(-\Gamma_e t) - E_h \exp(-\Gamma_h t)|^2. \quad (12)$$

This deviation is observed, and may be further explained by a distribution of levels in both the electron- and hole-

transport systems.³⁹

For the case of gratings written under the application of a high potential, the process would occur as follows. The electron-transport system establishes the initial space-charge field, while ambipolar diffusion establishes a complementary field at a lower rate. In this case, only the components of the space-charge gratings due to diffusion will be mutually screened as described above; that component due to drift will remain unscreened, and thus a hologram is initially observed. In a manner similar to the electron case, the net field is maintained at the same level, $E = -mE_0 = -mcE'_0$, according to photorefractive theory after Eq. (5), while the complementary gratings continue to grow. The decay process would follow the same sequence as the revelation process above, resulting first in the decay of the electron-created grating, revealing the hole-created grating, which then decays more slowly.

According to Eq. (5), the initial gratings established by electron drift are π -shifted with respect to the intensity pattern. Complementary gratings resulting from ambipolar diffusion are likely $(\pi/2)$ -shifted, as in the case of unipolar diffusion-only transport ($E_0 = 0$). The data show that the net grating does not always vanish completely prior to recovery; this observation may be explained by a phase difference between the principal and complementary space-charge fields, resulting from such details of the carrier-transport processes. Thus, the net space-charge field is indicated by

$$E_{SC}(t) = -E_e \exp(-\Gamma_e t + \delta_e) + E_h \exp(-\Gamma_h t + \delta_h), \quad (13)$$

where $E_e \geq 0$; $E_h \geq 0$; $0 \leq \delta_j < 2\pi$ for $j = e, h$; and $E_{SC}(0) = -mE_0$. Any nonzero difference in phase ($\delta_e - \delta_h$) results in a nonzero minimum during the revelation process.

The choice of 785-nm light is critical to the generation of complementary gratings in BSO and the decoupling of electron and hole transport; using the same crystal, no such behavior is observed with 514.5-nm light, but two-exponential decay is observed for gratings written with 514.5-nm light and erased with 820-nm light.¹⁵ The thermally-stimulated-current experiments outlined by Takamori and Just² have been performed on a BSO sample taken from the same boule as the sample used in this experiment, and similar trap levels have been identified. Thus, the two candidates for levels participating in two-level electron-hole transport described in Fig. 7 are the donor level at 2.6 eV and a trap at 1.4 eV or less, both measured from the bottom of the conduction band.

Using this model, 514.5-nm light excites electrons from both levels into the conduction band and also excites electrons from the valence band into both levels. For electron-dominated behavior, no complementary gratings form. For 785-nm light, whose corresponding energy is less than half the band-gap energy, the level closest to the conduction band contributes electrons to the space-charge grating and the level closest to the valence band contributes holes. Uniform illumination with 514.5-nm light serves to establish a nonequilibrium metastable oc-

cupation of the levels needed for the generation of complementary gratings. It is reasonable to expect that light of wavelength near or longer than 785 nm will contribute to the formation of complementary gratings, that light of wavelength near or shorter than 514.5 nm will not, and that light of wavelength in the middle of the range from 785 to 514.5 nm will show a transition range.

For both cases used to generate complementary gratings, the presence of an applied field during uniform illumination allows the revelation of the complementary gratings. The electric field decouples electron and hole transport, allowing the electron- and hole-formed gratings to decay independently. Without the electric field, normal decay occurs and complementary gratings are not revealed.

V. COMPARISON TO LITERATURE

Holograms are written in BSO with 785-nm light, but display certain recovery properties which can be explained by a two-level electron-hole-transport model. Kukhtarev *et al.*³⁴ and Valley³⁵ briefly evaluate the model, but limit their discussion to the diffusion case and draw no conclusions regarding the effect of high electric fields. The introduction and exposure of extended-lifetime complementary holograms is explained by extending the model.

Huignard and Herriau employ a multiple-step technique using 514.5- and 623.8-nm light to establish complementary extended-lifetime gratings in BSO in a different manner.^{4,16} In this case the space-charge grating is established using 514.5-nm light and a high electric field, $E'_0 = 6$ kV/cm. Then the 514.5-nm light is blocked. In the presence of the field, the net grating relaxes in the presence of 632.8-nm light, establishing a complementary grating. At this time, $E_e = E_h$. In a manner similar to the process outlined in this paper, revelation of the complementary grating occurs in the presence of the field under uniform illumination with 514.5-nm light. Attard observes similar effects.¹⁸

Strohkendl and Hellwarth write and erase gratings with 514.5-nm light and observe decay with a functional form of two exponentials.⁴⁰ Dube *et al.* have observed similar behavior in gratings written with 514.5-nm light and erased with 820-nm light.¹⁵ Baquedano *et al.* systematically study such multiple levels in BSO using variable-wavelength light for grating erasure.⁴¹ By writing gratings with 514.5-nm light and erasing the gratings with light between 390 and 620 nm, they observed two-exponential grating decay; by examining the details of the dependence of decay on erasure wavelength, they conclude that BSO has two centers, at 2.7 and 3.1 eV below the conduction band.

Kamshilin and Mitiva observe enhancement of grating transients in BSO by preillumination with filtered infrared light of 650–800 nm and grating formation using 488-nm light.¹² They present a model in which charge is pumped from one level to another during the preillumination phase, setting up a specific metastable population of states for subsequent charge redistribution.

Nolte *et al.* observe in semi-insulating InP a quenching of the photorefractive effect at low temperatures.³⁸ They

explain their observations using a multilevel electron-hole-transport model similar to that presented here. At room temperature, shallow traps are thermally emptied, and only one center contributes to the photorefractive effect by majority-carrier transport; at lower temperatures, however, shallow traps become populated and contribute to the screening of the photorefractive effect by minority-carrier transport. Thus, the quenching is a temperature-dependent screening of the principal grating by a superimposed complementary grating, and may be recoiled with the formalism developed here by assigning a temperature dependence to Γ_e , Γ_h , N^+ , N^- , P^+ , and P^- , and by including additional levels. The data on BSO presented here describe the role of an applied electric field in exposing the monitoring the time evolution of the complementary gratings.

VI. CONCLUDING REMARKS

The technique presented in this paper offers a relatively simple procedure for extending the readout time of holograms through the introduction of complementary holograms. No heating of the sample is required, as in the case of thermal fixing, and only one wavelength of monochromatic near-infrared light (785 nm) is needed. Ordinary lamps, ideally with some illumination in the near-ultraviolet spectrum, may also be used to erase the gratings.

Recently, Vainos *et al.* have observed semipermanent photochromic holograms in BSO.⁴² These holograms are written with high write-beam intensity and are erased only upon uniform heating at 300°C. Vainos *et al.* have also multiplexed semipermanent photochromic and real-time photorefractive holograms in BSO.⁴² Short-lived principal and long-lived complementary holograms described here might be multiplexed in a similar manner. Their relative phase could be controlled by placing a phase shifter in the path of the image beam shown in Fig. 1. Then a long-lived hologram would be written into the crystal with no applied electric potential and revealed with an applied potential. Next, while the potential is sustained, a second, short-lived hologram would be written into the crystal for the minimum time period needed to achieve saturation; this hologram will display little re-

velation behavior, and the extended-lifetime hologram will not be erased during this step. Thus, these two holograms are superimposed and have the same grating vector \mathbf{k} . Such multiplexing opens new possibilities for wavefront interferometry, image synthesis, logic operations, phase-object detection, holographic interferometry, and optical switching.⁴²

The species and concentrations of electron traps and donor centers involved in the photorefractive process at 785 nm have yet to be identified, and σ_e/σ_h has yet to be measured. Studies with variable wavelengths similar to those of Baquedano *et al.*⁴¹ may help resolve some of these issues. Temperature-dependent studies of the grating formation and decay characteristics would further aid in this identification process in BSO.⁴ Addition of impurities has been observed to alter physical processes^{1,3,15,25,43} and may be useful in optimizing this effect for a particular application. Additionally, introduction of impurities into GaAs and BaTiO₃ may lead to similar effects in these materials. Increased system sensitivity would allow monitoring of diffusion-field formation and revelation characteristics for weaker gratings resulting from shorter write times; it would also permit two-beam-coupling studies.

Although the response rate at 785 nm is lower than at 514.5 nm, the dipole lasers used are available quite inexpensively, promise to provide increased power output in the near future, and offer a compact illumination source. Furthermore, GaAs-based optoelectronic components have been integrated with other photorefractive materials;⁴⁴ BSO may also be suitable for integration with such optoelectronic devices, and the devices themselves may display similar effects.

ACKNOWLEDGMENTS

The authors thank R. G. Wheeler, R. K. Chang, K. Rabe, D. Just, A. P. Ghosh, and T. Takamori for helpful discussions. One of us M.C.B. gratefully acknowledges partial support by the IBM Corporation. This research has been supported in part by IBM Research Contracts No. 652916 and No. 12850046.

¹S. L. Hou, R. B. Lauer, and R. E. Aldrich, *J. Appl. Phys.* **44**, 2652 (1973).

²T. Takamori and D. Just, *J. Appl. Phys.* **67**, 848 (1990).

³N. Benjelloun, M. Tapiero, J. P. Zielinger, J. C. Launey, and F. Marsaud, *J. Appl. Phys.* **64**, 4013 (1988).

⁴A. Delboulbe, C. Fromont, J. P. Herriau, S. Mallick, and J. P. Huignard, *Appl. Phys. Lett.* **55**, 713 (1989).

⁵F. P. Strohkendal, *J. Appl. Phys.* **65**, 3773 (1989).

⁶See Refs. 1–5 for additional references therein.

⁷N. V. Kukhtarev, *Pis'ma Zh. Tekh. Fiz.* **2**, 1114 (1976) [*Sov. Tech. Phys. Lett.* **2**, 438 (1976)].

⁸N. V. Kukhtarev, V. B. Markov, S. G. Odulov, M. S. Soskin, and V. L. Vinetskii, *Ferroelectrics* **22**, 949 (1979).

⁹J. Feinberg, D. Heiman, A. R. Tanguay, Jr., and R. W.

Hellwarth, *J. Appl. Phys.* **51**, 1297 (1980).

¹⁰G. C. Valley, *IEEE J. Quantum Electron.* **QE-19**, 1637 (1983).

¹¹G. C. Valley and M. B. Klein, *Opt. Eng.* **22**, 704 (1983).

¹²A. A. Kamshilin and M. G. Miteva, *Opt. Commun.* **36**, 429 (1981).

¹³L. Arizmendi, *J. Appl. Phys.* **65**, 423 (1989).

¹⁴M. A. Powell and C. R. Petts, *Opt. Lett.* **11**, 36 (1986).

¹⁵R. R. Dube, D. Just, M. C. Bashaw, S. Mroczkowski, T.-P. Ma, and R. C. Barker, in *Nonlinear Optical Materials II*, edited by J.-B. Grun [*Proc. SPIE Int. Soc. Opt. Eng.* **1127**, 195 (1989)].

¹⁶J. P. Herriau and J. P. Huignard, *Appl. Phys. Lett.* **49**, 1140 (1986).

¹⁷A. E. Attard, *Appl. Opt.* **28**, 5169 (1989).

- ¹⁸A. E. Attard, *J. Appl. Phys.* **66**, 3211 (1989).
- ¹⁹N. A. Vainos, S. L. Clapham, and R. W. Eason, *Appl. Opt.* **28**, 4381 (1989).
- ²⁰D. L. Staebler and J. J. Amodi, *Ferroelectrics* **3**, 107 (1972).
- ²¹F. Micheron and G. Bismuth, *Appl. Phys. Lett.* **20**, 79 (1971).
- ²²F. Micheron, C. Mayeux, and J. C. Trotier, *Appl. Opt.* **13**, 784 (1974).
- ²³D. von der Linde, A. M. Glass, and K. F. Rodgers, *Appl. Phys. Lett.* **25**, 155 (1974).
- ²⁴D. von der Linde, A. M. Glass, and K. F. Rodgers, *Appl. Phys. Lett.* **26**, 22 (1975).
- ²⁵A. R. Tanguay, Jr., Ph.D. dissertation, Yale University, 1977.
- ²⁶A. R. Tanguay, Jr., S. Mroczkowski, and R. C. Barker, *J. Cryst. Growth* **42**, 431 (1977).
- ²⁷Because the coherence length of the diode laser used in these experiments varies with beam intensity and temperature, the modulation factor, m , is not a well-defined quantity. It is taken as constant over the time scales used in these experiments, 900 sec at the most. For erasure in the presence of uniform illumination, $m = 0$, and the coherence length is not a factor.
- ²⁸The write-read-erase process described here should be distinguished from two-beam coupling, in which energy is transferred from one beam to another during simultaneous illumination of the crystal by the beams.
- ²⁹R. A. Mullen, in *Photorefractive Materials and Their Applications I*, edited by P. Günter and J.-P. Huignard (Springer-Verlag, Berlin, 1988), p. 167.
- ³⁰J. M. C. Jonathan, R. W. Hellwarth, G. Roosen, *IEEE J. Quantum Electron.* **QE-22**, 1936 (1986).
- ³¹F. Vachss, Ph.D. dissertation, Stanford University, 1988, Chap. 3.
- ³²S. I. Stepanov, V. V. Kulikov, and M. P. Petrov, *Opt. Commun.* **44**, 19 (1982).
- ³³S. I. Stepanov and M. P. Petrov, in *Photorefractive Materials and Their Applications I*, edited by P. Günter and J.-P. Huignard (Springer-Verlag, Berlin, 1988), p. 263.
- ³⁴N. V. Kukhtarev, G. E. Dovgalenko, and V. N. Starkov, *Appl. Phys. A* **33**, 227 (1984).
- ³⁵G. C. Valley, *J. Appl. Phys.* **59**, 3363 (1986).
- ³⁶In this model, both levels are deep centers, rather than shallow traps, which are quickly thermalized. This condition permits the existence of a metastable state overall, in which both levels are partially occupied.
- ³⁷The superscripts represent the occupation state of a particular center, rather than its charge state. For example, if each of N is a donor center, then each of N^- is neutral and is occupied by an electron, and each of N^+ is positive and is empty (or occupied by a hole). Compensating ions allow for partial occupation of deep centers. Because the nature of the states in BSO is not well understood, the more general notation is used in this paper.
- ³⁸D. D. Nolte, D. H. Olson, and A. M. Glass, *Phys. Rev. Lett.* **63**, 891 (1989).
- ³⁹G. C. Valley, *Appl. Opt.* **22**, 3160 (1983).
- ⁴⁰F. P. Strohkendl and R. W. Hellwarth, *J. Appl. Phys.* **62**, 2450 (1987).
- ⁴¹J. A. Baquedano, L. Contreras, E. Diéguez, and J. M. Cabrera, *J. Appl. Phys.* **66**, 5146 (1989).
- ⁴²N. A. Vainos, S. L. Clapham, and R. W. Eason, *Appl. Opt.* **28**, 4386 (1989).
- ⁴³B. C. Grabmaier and Oberschmid, *Phys. Status Solidi A* **96**, 199 (1986).
- ⁴⁴See, for example, P. H. Beckwith and W. R. Christian, *Opt. Lett.* **14**, 642 (1989), and references therein for examples and proposals.

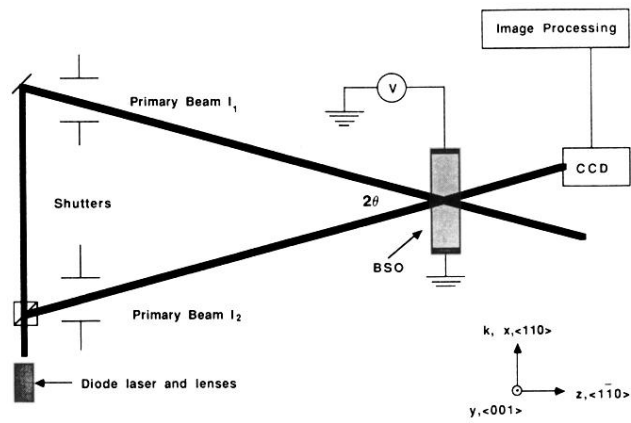


FIG. 1. Experimental arrangement for holographic recording in BSO at 785 nm. $I_1 = 665 \mu\text{W}/\text{cm}^2$ and $I_2 = 490 \mu\text{W}/\text{cm}^2$. Grating period $\Lambda = 10 \mu\text{m}$. $E'_0 = 0$ or 5 kV/cm. Note shown is a shutter-controlled 514.5-nm beam of an argon laser, incident on the surface of the crystal.